Jurnal Teknologi

Full paper

# Fixed-point Sensitivity Maps for Image Reconstruction in Tomography

Rahman Amirulah[a], Siti Zarina Mohd Muji[a*], Mohamad Hairol Jabbar[a], M. Fadzli Abdul Syaib[a], Ruzairi Abdul Rahim[b], Mohd Nasir Mahmood[c]

[a]*Embedded Computing Systems (EmbCoS) Research Focus Group, Computer Engineering Department, Faculty of Electrical and Electronic Engineering, Universiti Tun Hussein Onn Malaysia, 86400 Parit Raja, Batu Pahat, Johor, Malaysia*
[b]*Protom-I Research Group, Infocomm Research Alliance, Control and Mechatronic Engineering Department, Faculty of Electrical Engineering, Universiti Teknologi Malaysia, 81310 UTM Johor Bahru, Johor, Malaysia*
[c]*Language Academy, Universiti Teknologi Malaysia, 81310 UTM Johor Bahru, Johor, Malaysia*

*Corresponding author: szarina@uthm.edu.my

**Article history**

Received : 15 August 2014
Received in revised form :
5 January 2015
Accepted : 10 February 2015

**Graphical abstract**

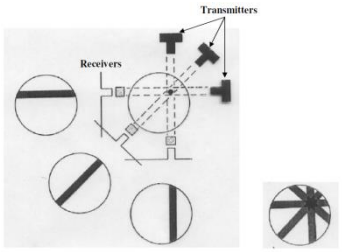


**Abstract**

This study proposes new fixed-point sensitivity maps for image reconstruction in optical tomography systems by using a linear back projection (LBP) algorithm. The projection selected is based on fan beam orientation with 16 pairs of transmitters and receivers. Many optical tomography systems previously published, focused on microcontroller implementations, which have limited processing speed for real time systems to be used in critical applications such as underwater gas transmission pipeline. To gain benefits from parallel processing in digital hardware implementations such as using FPGA or ASIC, slight modification must be done in the reconstructed images mechanism. The normalized sensitivity maps for image reconstruction are recreated without using floating numbers to optimize the digital design implementations. By multiplying the sensitivity maps matrix with 128, the new sensitivity maps matrices are developed and rounding processes are performed to eliminate floating numbers. The error was determined using Normalized Mean Square Error (NMSE) and the results show that the new fixed-point sensitivity maps produced comparable image reconstruction quality for optical tomography systems with NMSE values of $1.88 \times 10^{-7}$ and 0.02 for phantoms (a) and (b) respectively.

*Keywords*: Image reconstruction; optical tomography; fan beam; sensitivity maps



## 1.0 INTRODUCTION

Process tomography is a real-time imaging technique to visualize the dynamic flow characteristics of a moving object inside a vessel without invading the flow[1]. The real-time optical tomography systems developed by Ruzairi *et al.*[2] can be considered complicated because the systems need two data processing operations whereby the first is to capture the data and the other to reconstruct images. The data are then transferred from the first data processing operation into the second one in a local area network communication using WinSock programming function and switch box.

Tomography systems that use computers to reconstruct the images are called Computed Tomography (CT). This is because the tomography systems developed are using computers to reconstruct the images[2-7]. The hardware designs developed are call Data Acquisition Systems (DAS) that can be connected to the computers for data processing of image reconstruction. Figure 1 shows a typical computed tomography system developed previously.

The images that have been reconstructed using various tomographic sensing systems may contain important parameters in the cross-section of pipelines[8]. The parameters are either the velocity, flow rate, concentration profile or others[9].

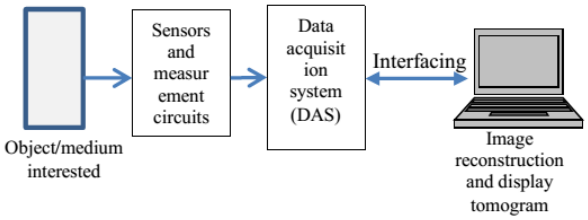


**Figure 1** Typical computed tomography system

Based on Siti Zarina *et al.*[10], Linear Back Projection (LBP) is the most widely used image reconstruction algorithm. The basic concept of LBP is concentration profile which is based on the multiplication of data projection from each sensor with the computed sensitivity maps[10]. Figure 2(a) shows the LBP concept with sensors arranged in fan beam projection. The results of the algorithm are the interception of the projection rays which will locate the object such as in Figure 2(b).

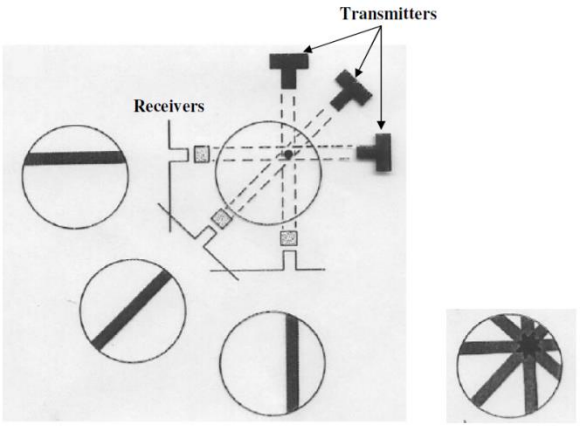


(a) (b)

**Figure 2** LBP and Fan Beam Projection, (a) LBP Concept, (b) Reconstructed Images

The reconstructed image is calculated based on Equation 1[11] where $V_{LBP(\overline{S})}(x,y)$ is voltage distribution using LBP algorithm, $V_{Tx,Rx}$ is sensor loss voltage of transmitter (Tx) and receiver (Rx) and $\overline{S}_{Tx,Rx}$ is normalized sensitivity map.

$$V_{LBP(\overline{S})}(x,y) = \sum_{Tx=1}^{16}\sum_{Rx=1}^{16} V_{Tx,Rx} \times \overline{S}_{Tx,Rx}(x,y) \quad \text{(Equation 1)}$$

The value of $V_{Tx,Rx}$ depends on the blockage along the pathway of the light projection. Let say there is an object blocking the pathway, then the amount of light received by the receiver is none. Thus, the voltage value is zero. With this value, the image pixels will be concentrating on zero which is the black colour in the image. Otherwise, if there is no object blocking the pathway, the maximum received voltage will be 5V. The 5V analogue voltage is converted into 8-bit digital value using ADC which provides $11111111_2$ (255). If the multiplication of Equation 1 is performed with the maximum value which is 1 for normalized sensitivity maps and the sensor loss voltage is 255. The result, 255, will produce the white colour in the images.

As for normalized sensitivity maps, they are created to be multiplied with the voltage loss value from the sensors. Sensitivity maps are a set of matrix that represents the pathway of the projection light from the transmitter to the receiver[12]. To develop the sensitivity maps, the dimensions of the sensor location are important where virtual projection is based on the identified projection pathway. In designing the projection pathway, four points are introduced for each of the 5mm size sensor. The projection pathway is based on equations as follow:

$$Position\ 0 = 16(Tn) \quad \text{(Equation 2)}$$
$$Position\ 1 = 16(Tn) + 2 \quad \text{(Equation 3)}$$
$$Position\ 2 = 16(Rn) + 6 \quad \text{(Equation 4)}$$
$$Position\ 3 = 16(Rn) + 8 \quad \text{(Equation 5)}$$
$$Position\ 4 = 16(Rn) + 10 \quad \text{(Equation 6)}$$
$$Position\ 5 = 16(Tn) - 2 \quad \text{(Equation 7)}$$
$$Position\ 6 = 16(Tn) \quad \text{(Equation 8)}$$

In these equations, $Tn$ represents the transmitters and $Rn$ represents the receivers and $n$ is the sensor numbers which are 0 to 15. For example, if the transmitter is $T1$ and the receiver is $R7$, then the position calculations are as follow:

$$Position\ 0 = 16(1) = 16$$
$$Position\ 1 = 16(1) + 2 = 18$$
$$Position\ 2 = 16(7) + 6 = 118$$
$$Position\ 3 = 16(7) + 8 = 120$$
$$Position\ 4 = 16(7) + 10 = 122$$
$$Position\ 5 = 16(1) - 2 = 14$$
$$Position\ 6 = 16(1) = 16$$

Based on the position values obtained, the pathway projections are drawn as in Figure 3 which represent sensitivity maps for Tx1 to Rx7. Since this work used 16 transmitters (Tx) and 16 receivers (Rx), thus there should be 256 sensitivity maps.

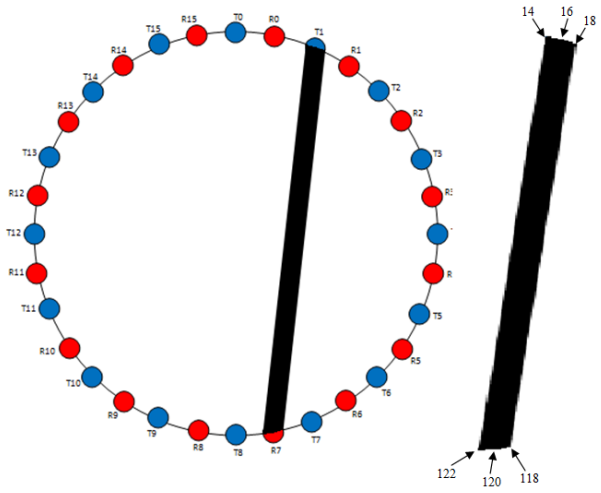


**Figure 3** Projection Pathways from Tx1 to Rx7

The sensitivity maps created are in the form of matrices with 64 rows and 64 columns. These 64 by 64 numbers represent the number of pixels of the reconstructed images. Therefore, the final image resulted will consist of 64 × 64 = 4096 number of pixels. Each pixel gives a different value due to the projection pathway[11]. The pixel values are calculated based on virtual projection shown in Figure 4 using Equation 9.

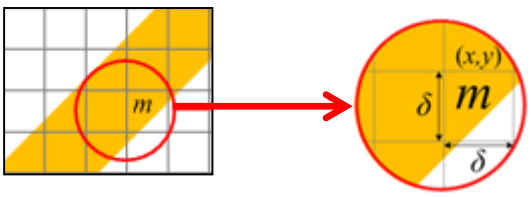


**Figure 4** Virtual Projection for pixels calculation

$$S_{Tx,Rx}(x,y) = \frac{m}{\delta^2} \quad \text{(Equation 9)}$$

Whereas $S_{Tx,Rx}$ $(x, y)$ is the sensitivity at position (x,y) (dimensionless), $m$ is the coloured pixel count occupied and δ is the rectangular pixel size. For example, let say the value of δ is 1mm and the value of $m$ is 40 from 64 of full coloured pixels. So, the value of $S_{Tx,Rx}$ $(x, y)$ calculated using Equation 9 will be 40.

In this case, the maximum value of each pixel is 64. Based on Equation 1, the sensitivity maps used are normalized sensitivity maps. To get the normalized sensitivity maps, Equation 10 is used. Each pixel value at the same position will be added to get the total value for all 256 sensitivity maps.

$$\overline{S}_{Tx,Rx}(x,y) = \frac{S_{Tx,Rx}(x,y)}{\sum_{Tx=0}^{15}\sum_{Rx=0}^{15} S_{Tx,Rx}(x,y)}$$

(Equation 10)

Whereas $\overline{S}_{Tx,Rx}(x,y)$ are the normalized sensitivity maps, $S_{Tx,Rx}(x,y)$ are the sensitivity maps for light projection of Tx to Rx and $\sum_{Tx=0}^{15}\sum_{Rx=0}^{15} S_{Tx,Rx}(x,y)$ is the summation of all sensitivity maps in the same pixel positions of x and y.

The normalized sensitivity maps calculated by using Equation 10 provide the pixel values in the range of 0 to 1 which are floating numbers. The floating numbers in the design are not easy especially for the digital design[13-14]. The processing of the fixed-point numbers in the digital design can quicken the development of a prototype of the systems because of less complexity. Thus, in order to quicken the prototyping of the digital system design and to reduce the complexity of the calculation process, new sensitivity maps without floating points are required. Therefore, this problem provides a new opportunity in developing the fixed-point sensitivity maps. It is expected that the new fixed-point sensitivity maps are able to reconstruct the images as good as the normalized sensitivity maps.

## ■2.0 PROPOSED FIXED-POINT SENSITIVITY MAPS

By using MATLAB, all the normalized sensitivity maps are reproduced. In order to terminate the floating point numbers in the normalized sensitivity maps, the normalized sensitivity maps pixel values are multiplied with 128. The value of 128 was chosen as the multiplicand because the binary number is $10000000_2$ which is not more than 8-bit, such that the memory capacity requirement for hardware implementation can be reduced. As explained before, the value of normalized sensitivity maps are between 0 to 1. Thus the maximum value after the multiplication is 128. The multiplication process is calculated using Equation 11 as follows:

$$SM_{Tx,Rx}(x,y) = \overline{S}_{Tx,Rx}(x,y) \times 128 \quad \text{(Equation 11)}$$

Whereas $SM_{Tx,Rx}(x,y)$ are the new sensitivity maps, $\overline{S}_{Tx,Rx}(x,y)$ are the previous values of normalized sensitivity maps.

However, after the multiplication process of normalized sensitivity maps with 128, the new results of sensitivity maps multiplications still have floating point numbers. For example, let say the normalized sensitivity map pixel value is 0.2245. Once multiplied with the constant 128, the result is 28.736 which is still a floating number. To get the fixed-point number, the new multiplied sensitivity map value is rounded by using MATLAB software, and the final new sensitivity map is 29 for the normalized sensitivity map of 0.2245. Thus, based on Equation 11, all the 256 sensitivity maps pixel values are multiplied and the pixel values are also rounded for the fixed-point.

Once all the processes of calculation for the new sensitivity maps $SM_{Tx,Rx}(x,y)$ were completed, the image reconstruction process is performed by using Equation 12.

$$V_{LBP(SM)}(x,y) = \sum_{Tx=1}^{16}\sum_{Rx=1}^{16} V_{Tx,Rx} \times SM_{Tx,Rx}(x,y)$$

(Equation 12)

Based on Equation 12, the results raise a new problem due to the new fixed-point sensitivity maps. For example, if the maximum values of the sensor loss voltage $V_{Tx,Rx}$ and the sensitivity maps are 255 and 128 respectively, the multiplication result will be 32640 in each pixel. The images reconstructed in this study are in the range of 0 to 255 for the pixel values. Therefore, to get back the values with the range of 0 to 255, the multiplication results must be divided by 128. The final reconstructed pixel values are calculated using Equation 13 such that the image reconstructed pixel values are limited to a maximum of 255.

$$V_{LBP(SM)}(x,y) = \frac{\sum_{Tx=1}^{16}\sum_{Rx=1}^{16} V_{Tx,Rx} \times SM_{Tx,Rx}(x,y)}{128}$$

(Equation 13)

The experiment was carried out based on two phantom input data which are shown in Figure 5.

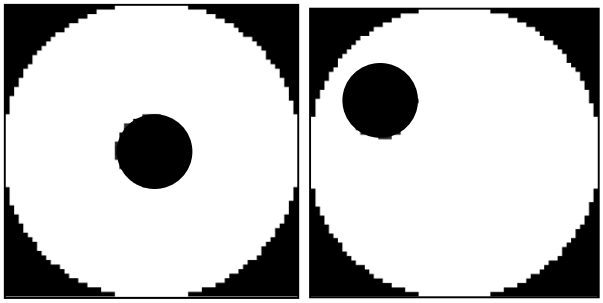

(a) (b)

**Figure 5** Input Data: (a) Phantom at the center of the pipe and (b) Phantom at the edge of the pipe

The process flow to reconstruct the images in this study is shown in pseudo code as follows:

```
Start
    Load Input Data Phantom (a) or (b)
    Load Sensitivity Maps Matrices
    for x = 1 to 64
        for y = 1 to 64
            Calculate V_LBP(S̄)(x,y) or V_LBP(SM)(x,y)
        end for
    end for
    Combine V_LBP(S̄)(x,y) or V_LBP(SM)(x,y)
    Display Tomogram
End
```

The reconstructed images using these new fixed-point sensitivity maps are compared with the previous images reconstructed using normalized sensitivity maps. The error was determined and calculated using Normalized Mean Square Error (*NMSE*) based on Equation 14. The NMSE in Equation 14 can be used to improve the quality of the images[15]. The equation will determine the difference between the images reconstructed in $V_{LBP(\overline{S})}(x,y)$ and $V_{LBP(SM)}(x,y)$ based on $V_{LBP(\overline{S})}(x,y)$ as the original images reconstructed using normalized sensitivity maps.

$$NMSE = \frac{\sum_{x=1}^{64}\sum_{y=1}^{64}\left[V_{LBP(\overline{S})}(x,y) - V_{LBP(SM)}(x,y)\right]^2}{\sum_{x=1}^{64}\sum_{y=1}^{64}\left[V_{LBP(\overline{S})}(x,y)\right]^2}$$

(Equation 14)

## 3.0 RESULTS AND DISCUSSION

The primary aim of this experiment is to investigate whether the new fixed-point sensitivity maps are able to produce the reconstructed images as good as the previous floating sensitivity maps.

Based on the two input data phantoms, the results of the images reconstructed were visualized and tested. For phantom (a), the image reconstructed is shown in Figure 6 whereas Figure 6(a) is the previous normalized sensitivity map with floating pixel numbers and Figure 6(b) is the new fixed-point sensitivity map.

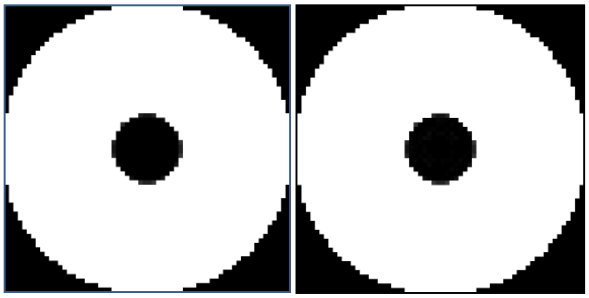

(a) (b)

**Figure 6** Reconstructed Images for Phantom (a)

From visual inspection of the images reconstructed in Figure 6, both have the same shapes and number of pixels that display the circle in the middle. By using NMSE, the calculated error is very small, which is $1.88 \times 10^{-7}$.

Figure 7 shows the images reconstructed for phantom (b). It is clearly shown that the shapes are slightly different for a few pixels; however both images show that the position of the phantom is correct for both reconstructed images. Based on the NMSE analysis, the error value calculated for phantom (b) is 0.02, which is still acceptable.

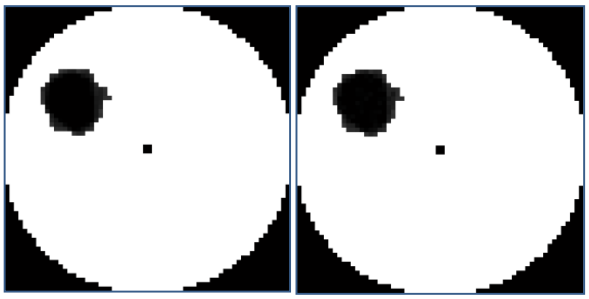

(a) (b)

**Figure 7** Reconstructed Images for Phantom (b)

## 4.0 CONCLUSION

As a conclusion, the study has proposed a new fixed-point sensitivity maps for optical tomography system to be targeted for digital hardware implementation to be benefitted from the parallel processing capability. Experimental results have demonstrated that the images were reconstructed based on proposed fixed-point sensitivity maps using linear back projection (LBP) algorithm which are comparable to floating-point sensitivity maps. By using NMSE, the results are $1.88 \times 10^{-7}$ and 0.02 for phantoms (a) and (b) respectively. Therefore, the proposed fixed-point sensitivity maps are more suitable for digital hardware implementations such as in FPGA or ASIC because of less complex computation compared with floating-point normalized sensitivity maps. Another advantage of using fixed-point sensitivity maps is that they need less memory capacity requirement in order to store the sensitivity maps matrix data.

## Acknowledgement

The authors would like to thank the Ministry of Higher Education and Universiti Tun Hussein Onn Malaysia for supporting this research under Research Acculturation Collaborative Effort (RACE) vot number 1120.

## References

[1] M. Fadzli, *et al.* 2012. A Study on Optical Sensors Orientation for Tomography System Development. *Sensor & Transducers Journal*. 140(5): 45–52.
[2] Ruzairi Abdul Rahim, *et al.* 2011. Optical Tomography: Real-time Image Reconstruction System using Two Data Processing Units. *Jurnal Teknologi*. 55(Sains & Kej) Keluaran Khas (2): 63–73.
[3] S. Z. M. Muji, *et al.* 2013. Optical Tomography Hardware Developmentfor Solid Gas Measurement using Mixed Projection. *Flow Measurement ans Instrumentation*. 33: 110–121.
[4] Ruzairi Abdul Rahim, *et al.* 2013. Hardware Design of Laser Optical Tomography System for Detection of Bubbles Column. *Jurnal Teknologi (Sciences & Engineering)*. 64(5): 69–73.
[5] Ruzairi Abdul Rahim *et al.* 2014. A Review of Process Tomography Application in Inspection System. *Jurnal Teknologi (Sciences & Engineering)*. 70(3): 35–39.
[6] Ruzairi Abdul Rahim *et al.* 2014. A Review of Optical Tomography System. *Jurnal Teknologi (Sciences & Engineering)*. 69(8): 1–6.
[7] Wei Mingsheng, *et al.* 2012. Detection of Coal Dust in a Mine Using Optical Tomography. *International Journal of Mining Science and Technology*. 22: 523–527.
[8] R. A. Williams and M. S. Beck. 1995. *Process Tomography: Principles, Techniques, and Applications*. Butterworth-Heinemann Ltd. 624.
[9] M. T. M. Khairi, *et al.* 2012. A Review on Application of Optical Tomography in Industrial Process. *International Journal on Smart Sensing and Intelligent Systems*. 5(4): 767–798.
[10] Siti Zarina Mohd Muji, *et al.* 2011. Optical Tomography: A Review on Sensor Array, Projection Arrangement and Image Reconstruction Algorithm. *International Journal of Innovative Computing, Information and Control*. 7(7(A)): 3839–3856.
[11] Mohd Hafiz Fazalul Rahiman, *et al.* 2014. A Study on Forward and Inverse Problems for an Ultrasonic Tomography. *Jurnal Teknologi (Sciences & Engineering)*. 70(3): 113–117.
[12] Ruzairi Abdul Rahim *et al.* 2014. Octagon Modelling Using Parallel Projection of Optical Tomography. *Jurnal Teknologi (Sciences & Engineering)*. 70(3): 25–28.
[13] Miriam Leeser, *et al.* 2005. Parallel-Beam Backprojection: An FPGA Implementation Optimized for Medical Imaging. *Journal of VLSI Signal Processing System for Signal, Image and Video Technology*. 39(3): 295–311.
[14] Gene Frantz and Ray Simar. 2004. *Comparing Fixed-Point ans Floating-Point DSPs*. Texas Instruments. 1–7.
[15] Jacub Peksinski, *et al.* 2012. *Syncronization of Two Dimensional Digital Images Using NMSE Measure.* 35th International Conference on Telecommunications and Signal Processing (TSP). 710–714.